Meridional circulation and transports in ORCA025 climatological experiments

A.M. Treguier [*], J.M.Molines [†], Gurvan Madec [‡]

Laboratoire de Physique des Oceans report LPO-06-02, March 2006

1 Introduction and model description

This report contributes to the preliminary validation of the ORCA025 configuration of the DRAKKAR project (www.ifremer.fr/lpo/drakkar). Only experiments forced by a repeated seasonal cycle forcing are considered here. Most of the plots are for the global ocean but some emphasize the Southern Ocean.

The model (ORCA025) is the 1/4 ° global configuration of the DRAKKAR project. It uses the NEMO system: OPA9 coupled with the LIM sea ice model, www.lodyc.jussieu.fr/NEMO. The configuration is described in Barnier *et al.* (2006). The main experiment considered here, ORCA025-G42, is short: it lasts 10 years. It starts from rest with initialization to Levitus/PHC climatology. The model is forced using atmospheric variables and calculating fluxes with bulk formulae. The CORE forcing fields (Large and Yeager, 2004) are taken from the GFDL web site. We use the so-called "normal year" forcing, which is in fact year 1992 but corrected so as to resemble the average of the NCEP period 1958-2000. Air temperature, humidity and winds are taken from NCEP (with corrections) but radiative fluxes are from satellite observations. The forcing files have been interpolated by Laurent Brodeau (LEGI, Grenoble) using his fortran interpolation package

[*]Laboratoire de Physique des oceans, CNRS-Ifremer-UBO, Brest, France

[†]Laboratoire des Ecoulements Geophysiques et Industriels, Joseph Fourier University, Grenoble, France

[‡]LOCEAN, Paris,France

(Brodeau, 2004). Bulk formulae are the NCAR version provided with the CORE forcing. Our inputs are daily wind speed, air temperature, and humidity; daily short wave and long wave radiation, and monthly rain and snow precipitations. We do not use the sea level pressure (we keep the sea level pressure constant in the bulk formulae). Runoffs include the major rivers calculated by Edmee Durand at MERCATOR for the first POG version (in 2003), with some coastal runoffs added by A.M. Treguier from the Dai and Trenberth (2002) database but this file has been done in a quick and dirty fashion (some rivers may end up counted twice). An updated runoff file is now available for the next runs. The total runoff is about 1.2 Sv. The model was run on 186 processors of the IDRIS computer centre IBM SP3 by Jean Marc Molines (Grenoble). We consider here the last three years. The time-mean transport in Drake Passage is 124 Sv. the transport between Australia and Antarctica is 143 Sv, the difference being the sum of the Bering transport (1 Sv) and Indonesian Throughflow (18 Sv).

We sometimes compare the ORCA025-G42 experiment with ORCA025-G32, of the same duration but using a different forcing (a mixture of NCEP climatology, other climatologies, NCEP average air temperature over the years 1992-2000 and observed ERS wind stress averaged over the period 1992-2000). G32 also uses different bulk formulae (CLIO bulk). The ACC transport is larger in ORCA025-G42 (Drake: 144 Sv, Australia: 165 Sv) probably because the wind stress, representative of recent years, is larger.

2 Meridional overturning in z-coordinates

Fig.1 shows meridional overturning in z-coordinates. Compared with the global model of Maltrud *et al.*(2005), which is run for a similar length of time (15 years), ORCA025-G42 is characterized by a weak Atlantic cell (10 Sv at 30°S vs 16 Sv for Maltrud *et al.*, their Fig 2a), and a stronger Indo-Pacific deep cell (20 Sv at 30°S vs 14 Sv for Maltrud *et al.*, their Fig 2b). The strength of the Deacon cell in the Southern ocean varies like the Ekman transport (Fig.2). Experiment G32 with a higher Ekman transport also has a larger Deacon cell (over 24 Sv).

The strength of the Atlantic overturning at 40°N depends on the forcing: it is much higher in G32 (22 Sv) than in G42 (14Sv). The large (and growing) value in G32 does not happen for the right reasons (a new dense, warm and saline water mass is being formed in the Nordic Seas and flowing through Denmark Strait). ORCA025-G42 has a more classical behavior for a z-coordinate model with a loss (mixing) of dense water downstream of the Nordic sills. The CORE forcing

does not seem to promote large values of the Atlantic overturning in the North Atlantic. Considering the South Atlantic (30°S), it is unclear what influences the Atlantic overturning there. It varies little between our runs (10 Sv in G42, 12 Sv for G32), but it is 16 sv for Maltrud *et al.*. The same applies to the Indo-Pacific deep cell (20 Sv in G42 and 22 Sv in G32).

3 Meridional overturning in σ_2-coordinates

The overturning in density coordinates (Fig.3) has an eddy contribution (Fig.5), which has been evaluated recently in the global OCCAM model by Lee and Coward (2003). The maximum eddy transport in ORCA025 is larger (10 Sv rather than 6 Sv for OCCAM). It acts in the same way: poleward transport for waters less dense than $\sigma_2 \approx 37$, and equatorward transport below (in the sense of flattening the isopycnals).

The Deacon cell does not appear in the density coordinates overturning. Its cancellation in the zonal average does not depend on eddies, as shown by the relatively small difference between Figs 3 and 4 (same as found by Lee and Coward). The mechanism of cancellation, explained by Doos and Webb (1994) is that of vertical compensation between water flowing north at a given density and water flowing south at the same density, but deeper. At 50°S we find that the near-surface transport of about 20 Sv in the z-coordinate view (Fig 1) is replaced in the density view (Fig.3) by a southward transport in the lighter waters. This happens because there is a significant gradient of density along a latitude line (Fig.6 shows the 50°S section). The lighter isopycnals are present only in part of the Pacific, and the northward Ekman transport there is balanced by southward transport at greater depths, or in intense and deep current fronts, so that the net transport above isopycnal 35.8 at 50°S is 10 Sv poleward. This means that the zonal average cannot give us information about the "diabatic Deacon cell" (Speer *et al.*, 2000): an average following contours of surface density would be needed to expose this circulation.

Although eddy effects are similar, the mean overturnings of ORCA025-G42 and OCCAM are different. One difference is that in OCCAM everything seems shifted towards higher densities (or equivalently, isopycnals seem shifted down). This is because the density coordinate used in OCCAM was referenced to 1940 m, corresponding to a model level, rather than 2000 m (Mei Man Lee, personal communication): this shift is purely diagnostic and has nothing to do with model dynamics, unlike the difference in structure describe hereafter.

The meridional circulation at 30 °S in models is usually made of three cells, as found in FRAM (Doos and Webb, 1994), OCCAM (Lee and Coward, 2003) and numerous other low resolution models (a recent ORCA2 run, for example). The bottom cell reflects the circulation of the Pacific and Indian ocean and consists of bottom and lower deep water flowing north and returning at a lower depth. The second cell reflects the Atlantic circulation: it involves dense water that sinks in the Northern hemisphere, flows southwards, upwells in the ACC and returns North as upper deep water. The upper (subtropical) cell extents as far south as 30-40S in the zonal average; it is made of upper layer water moving south, being converted to lower densities and returning north (as intermediate water? subantarctic mode water?). Because the Atlantic cell is relatively weak in ORCA025 and the Indo-Pacific cell is large, only two cells appear at 30°S in the zonal average. This does not seem in contradiction with inverse solutions such as Sloyan and Rintoul or Talley et al (2003). The deep cell in the model is 24 Sv, in agreement with Ganachaud and Talley's inversions rather than Sloyan and Rintoul's (who have 50 Sv). The upper cell is strong (32 Sv at 15°S), as usual in high resolution models. Its strength of about 12 sv at 30°S is in agreement with Talley (her fig 4). 6 Sv of water upwell from the deep to the upper cell.

4 Model drift

The overturning itself does not vary much between year 2 and the last 3 years, excepted near 60°S at densities larger than 37 where a strong cell is found in year 2 and not later (Fig.7). The drift in properties needs to act on longer time scales to affect the global overturning circulation.

The zonally averaged differences with the Levitus climatology are represented in Figs.8, 9 and 10 for the temperature, salinity and density σ_2 respectively. The model temperature has increased everywhere south of 50°S, with maximum warming around 100 m reaching 1.6°C. This warming in the upper layer is due to the upward shift of the temperature minimum (Fig.11). It is located below 100 m depth in the climatology but near 50 m in the model. The model salinity increases in the intermediate water, decreases below down to about 2000 m, and increases slightly in the deeper layer (Fig.9). The net result is a decrease in density everywhere south of 50°S, excepted near 50 m depth because of the appearance of a temperature minimum there and the increase of salinity. The drifts are of the same order of magnitude in the two experiments with different forcing fields, but details differ. ORCA025-G42 with CORE forcing maintains a temperature mini-

mum at high latitudes (albeit at the wrong depth) while ORCA025-G32 does not. In the band 70°S to 60°S from 200 m to 3000 m depth, ORCA025-G42 has a warming reaching about 0.3°C at 1000 m. ORCA025-G32 has a cooling there, reaching -0.5°C at 1000 m. Combination of the cooling and salinity increase in ORCA025-G32 results in less drift in density south of 50°S.

Lee *et al.* (2002) quantify the drift by the variation in depth of isopycnals. Our calculation (Fig.12) shows a different pattern (compare with their Fig. 3) but overall agreement: in the deep layers south of 60°S isopycnals move down at a rate greater than 25 m/year. Lee *et al.* (2002) also calculate an integral of the volume drift that can be compared to the meridional overturning (Fig. 13, to be compared with their Fig. 5). Lee *et al.* (2002) find a loss in bottom water at a rate of 20 Sv south of 50°S very similar to our result. This is a large drift which renders difficult the interpretation of the meridional circulation in terms of water mass formation. It is interesting that the drifts in OCCAM and ORCA025 are so similar while the meridional streamfunctions in density coordinates are quite different.

5 Freshwater, heat and salt transports

This section is an attempt at estimating water, heat and salt balances in the model, and assess the validity of the database (5-days averages) to do such a calculation. Because of the free surface condition it is more complicated than in a rigid-lid model.

Let us first consider the balance of total water. In the time mean, the surface E-P-R flux must be compensated by a meridional transport of water, or by a drift of the sea surface height η. Fig.14 shows the global integrated volume transport,

$$\int_{-H}^{0} \int_{x} \overline{v}(x,y,z)\,dx\,dz.$$

The amplitude and shape are reasonable compared with estimated of the global freshwater transport (Wijffels, 2001). The model transport is very close to the transport implied by the E-P-R flux, when the global imbalance of the flux is removed (the curves would not be distinguishable on this figure). The difference is 1% at most. However, when we consider the total flux (without removing the global average) there is a significant imbalance (Fig.15). It should be equal to the drift in volume due to the variation in sea surface height (SSH). During the three years, the effect of the surface fluxes is 0.169 Sv, and the SSH increase

(an elevation gain of 4.5 cm) corresponds exactly to 0.169 Sv when using the last shapshot of years 10 and year 7. However, the spatial structure of $\partial - t\eta$ is dominated by mesoscale features, and the spatial average of the drift depends on which snapshot is used. For example if we take the last snapshot of year 10 and the first of year 8, we get an imbalance of 2.5%. For exact results the restart files corresponding to the beginning and end of the period should be used.

Following the notations of Roullet and Madec (2000, hereafter RM), the temperature equation can be written:

$$\partial_t T = -\nabla(T\mathbf{u}) + D_T + F_T \delta(k=1)$$

T is the temperature, $\mathbf{u}$ the three dimensional velocity, and D_T the diffusion. Although the surface flux is actually entered in the model as a boundary condition on the vertical diffusion operator, we write it here separately for clarity (with a δ function as it enters only the top layer:

$$F_T = \frac{Q}{\rho C_p h_1},$$

with Q the surface heat flux (in W.m^{-2}), ρ and Cp are a constant density and heat capacity, and h_1 is the thickness of the top layer (constant because of the linearized free surface formulation). There is no additional heat flux associated with the concentration/dilution effect because the temperature of the precipitation, evaporation and runoffs is taken to be equal to the sea surface temperature (see comments of routine trasbc). Following RM, we would say that the forcing on temperature associated with the water flux is zero because the dilution effect exactly balances the direct effect. When integrating the temperature equation over a volume to calculate the heat balance, we integrate over a fixed volume because of the linearization of the free surface (RM, paragraph 2.3). Integrating northward from Antarctica ($y = -80$) to a latitude y, we obtain:

$$\begin{aligned} \rho C_p \int_{-80}^{y}\int_{-H}^{0}\int_x \partial_t T\, dx dy dz + \rho C_p \int_{-H}^{0}\int_x V.T\, dx dz \quad + \\ \rho C_p \int_{-80}^{y}\int_x wT(z=0)\, dx dy - \int_{-80}^{y}\int_x Q\, dx dy \quad = \quad 0 \end{aligned} \tag{1}$$

On the lhs, the first term is the heat content drift and the second term the meridional heat transport. The third term would be zero in a rigid lid model. Using the expression for w in the linearized free surface case (RM), we get:

$$wT = T\partial_t \eta + T(E - P - R).$$

The second term has a physical meaning: it it the heat flux associated with the evaporation, precipitation and runoff. The first term is a consequense of linearizing the free surface. In a fully nonlinear free surface, this term would be balanced by an additional heat content drift associated with integrating the temperature over a variable volume. The global meridional heat transport is presented in Fig.16 for ORCA025-G42. At first order, it is equal to the transport implied by the surface fluxes (thin black curve, last term in (1)). The eddy contribution represents about half the total heat transport at 40°S, but is more modest at 50°S. Both the pattern and amplitude of the eddy transport are in agreement with the values of Jayne and Marotzke (2002) calculated from a lower resolution model. Jayne and Marotzke show that the large eddy transport occurs mainly in the Agulhas and the Indian ocean subtropical front. The eddy contribution is relatively smaller in the ACC itself, south of 40°S . This is to be expected because time-mean meridional excursions ('standing eddies') are always found to dominate transient eddy fluctuations in the zonal average (this is also true for momentum balances). The wT term (Fig.16) is rather small compared to the meridional transport, but must be taken into account because its global integral is non-negligeable (0.09 Pw). Its decomposition following (5) is shown in Fig.17. The residual flux due to the linearization of the free surface is small. Its global integral (0.016 Pw) is approximately equal to the product of the average sea surface temperature (T = 18.39) and the drift of the mean sea surface (0.045 m over 3 years) integrated over the domain and multiplied by ρC_p. In Fig.18 we consider how the flux terms balance the heat content drift. There is some local imbalance, probably due to the diffusive flux that has not been estimated. The global integrated heat balance is given in Table 1: there is a net cooling by the surface flux of -0.273 Pw, and a contribution of -0.077 Pw from (E-P-R), balancing a drift due to SSH (0.016Pw) and a decrease of heat content in the fixed volume (-0.365 Pw). The residual is 0.001 Pw. This good agreement may be somewhat fortuitous, since as in the case of η the estimation of the drift from 5-day averages is not completely reliable. Differences of up to 5% arise by taking different snapshots. It would probably be more accurate to calculate the diffusive flux; the drift could then be estimated as a residual rather than directly. The heat input by the surface flux (-0.273 Pw) corresponds to a spatially averaged flux of -0.76 W.m^{-2}.

Let us consider the equation for salinity S with similar notations as (5):

$$\partial_t S = -\nabla(S\mathbf{u}) + D_S + S(z=0)(F_i + E - P - R)/h_1\delta(k=1).$$

There is no external flux of salt ($F_S = 0$), but there is an important dilution effect since the salinity of evaporation, precipitation and runoff is taken to be zero. There

is also an ice-ocean flux F_i. Integrating to get a salt balance:

$$\int_{-80}^{y}\int_{-H}^{0}\int_{x}\partial_t S\,dx\,dy\,dz+\int_{-H}^{0}\int_{x}V.S\,dx\,dz+\int_{-80}^{y}\int_{x}wS(z=0)\,dx\,dy \\ -\int_{-80}^{y}\int_{x}S(z=0)(F_i+E-P-R)\,dx\,dy=0 \qquad (2)$$

Using the expression for w, the sum of the last two terms reduces to:

$$\int_{-80}^{y}\int_{x}wS(z=0)\,dx\,dy-\int_{-80}^{y}\int_{x}S(F_i+E-P-R)\,dx\,dy= \\ \int_{-80}^{y}\int_{x}\partial_t\eta S(z=0)\,dx\,dy-\int_{-80}^{y}\int_{x}F_iS(z=0)\,dx\,dy. \qquad (3)$$

For conservation of total salt in the ocean, those two terms should average to zero globally. As was the case for the heat balance, the first term on the rhs is a consequence of the linear free surface (RM showed it to be small in the global average for an equilibrated ORCA2 run). In our case this term is not small due to the drift of the mean SSH. The mean surface salinity being 34.6, a drift of 0.173 Sv in SSH produces a change in salt content at a rate of 6 Sv.PSU, which almost totally explains the decrease of the global mean salinity (-4.10^{-4} PSU) during the three years.

The meridional salt transport is presented in Fig.18. Separation between eddy and mean components shows a large cancellation between the two at 40°S. Our estimates agree qualitatively with Meijers *et al.* (2006), who used a model with similar resolution. The eddy freshwater transport is largest at 40°S as was the case for the heat transport. We have also plotted on this graph the transport implied by the ice-ocean flux F_i. This transport is almost zero in the global average, which is ensured by using a constant salinity of 34.7 instead of the actual sea surface salinity in forcing of the salinity equation. It seems that a large part of the meridional transport of salt at high latitudes is balanced by the ice-ocean surface forcing. In Fig.19 we consider the global salt balance. The non-conservation of salt in the fixed volume results from the drift in sea surface height, which makes the wS term to be different from the surface flux term in (2), as shown in the top panel. In the bottom panel this imbalance is compared to the drift in salt content in the fixed volume. In the global mean there is a very good agreement: the residual due to sea surface drift is 6.19 Sv.PSU, and the salt content drift is 6.09 Sv.PSU. The difference is large locally at certain latitudes, but this again is probably the effect of the diffusive salt flux along isopycnals which has not been calculated here. Note

that simply taking the product of the sea surface height drift (0.169 Sv) with the averaged surface salinity (34.6 PSU) is 5.8 Sv.PSU, which is a good first order estimate of the SSH-induced salinity drift. This drift represents a decrease of the global mean salinity of 4.10^{-4}PSU in the fixed volume over the three years.

When the total salt content is estimated taking into account the sea surface contribution:

$$\int_{-80}^{y}\int_{-H}^{0}\int S dx dy dz + \int_{-80}^{y}\int S\eta\, dx dy$$

this quantity is be conserved to a very good approximation (0.1 Sv.PSU), which results from the fact that there is no flux of salt through the ocean surface. It is not true for temperature, because most of the drift is due to the direct heating which is non-zero in the global average.

6 References

Barnier, B., G. Madec, T. Penduff, J.M. Molines, A.M. Treguier, A. Beckmann, A. Biastoch, C. Boening, J. Dengg, S. Gulev, J. Le Sommer, E. Remy, C. Talandier, S. Theetten, M. Maltrud, J. McClean, 2005: recent progress in modelling the global ocean at eddy permitting resolution. submitted to Ocean Dynamics.

Brodeau, L, 2004: A comparison between two interpolation tools. Drakkar report, available at www.ifremer.fr/lpo/drakkar

Doos, K., and D. J. Webb, 1994: The Deacon cell and the other meridional cells of the southern ocean. *J. Phys. Oceanogr.*, 24, 429-442.

Large, W., and S. Yeager, 2004: Diurnal to decadal global forcing for ocean and sea-ice models: the datasets and flux climatologies. NCAR technical note: NCAR/TN-460+STR, CGD division of the National Center for Atmospheric Research.

Lee, M.M., and A Coward, 2003: Eddy mass transport for the Southern Ocean in an eddy-permitting global ocean model. Ocean Modelling, 5, 249-266.

Maltrud, M.E., and J.L. McClean, 2005: An eddy resolving global 1/10 ocean simulation. Ocean Modelling, 8, 31-54.

Lee, M.M., A. Coward, and J. G. Nurser, 2002: Spurious diapycnal mixing of the deep waters in an eddy-permitting global ocean model. J. Phys. Oceanogr, 32, 1522-1535.

Meijers A. J.ł, N. L. Bindoff, J. L. Roberts, 2006: On the total, mean and eddy heat and freshwater transports in the Southern Hemisphere of a $1/8^\circ \times 1/8^\circ$ global ocean model. Submitted to ...

Roullet, G., and G. Madec, 2000: Salt conservation, free surface and varying levels: a new formulation for an ocean GCM. J. Geophys. Res., 105, 23927-23942.

Sloyan, B.M., and S.R. Rintoul, 2001: The southern ocean limb of the global deep overturning circulation, J. Phys. oceanogr., 31, 143-173.

Speer, K., S.R. Rintoul, B. Sloyan, 2000: The diabatic Deacon cell. J. Phys. Oceanogr., 30, 3212-3222.

Wijffels, S. 2001: Ocean Transport of Fresh Water. In: Siedler, G., Church, J. and Gould, J. (eds.). Ocean Circulation and Climate: Observing and Modelling the Global Ocean. Academic Press: pp

Term	Total (Pw)	Average ($W.m^{-2}$)
Surface heat flux	-0.273	-0.76
E-P-R heat flux	-0.076	0.046
Volume drift	-0.364	-1.01
SSH drift	0.016	0.045
Residual	0.001	0.003

Table 1: Global heat balance in ORCA025-G42

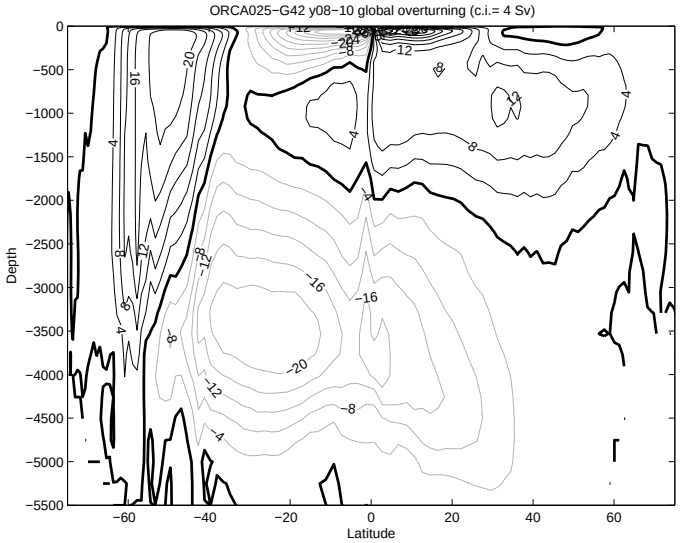

Figure 1: Global overturning in z-coordinates for the average of years 8-10 of ORCA025-G42. Negative contours are grey.

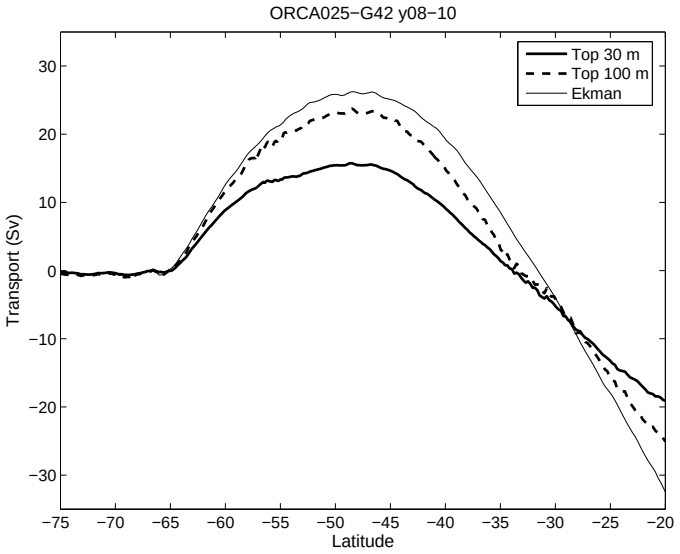

Figure 2: Comparison of the meridional transport integrated from the surface in ORCA025-G42 with the Ekman transport.

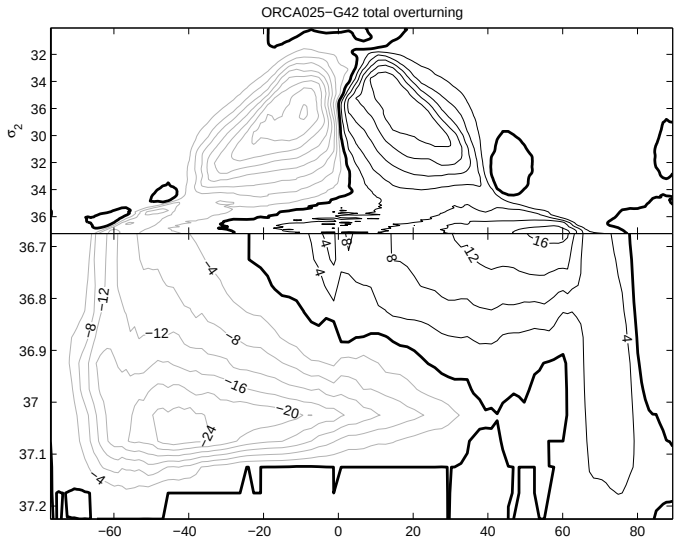

Figure 3: Global overturning (Sv) in σ_2-coordinates averaged over years 8-10 of ORCA025-G42. It is calculated from 5-days means. Negative contours are grey.

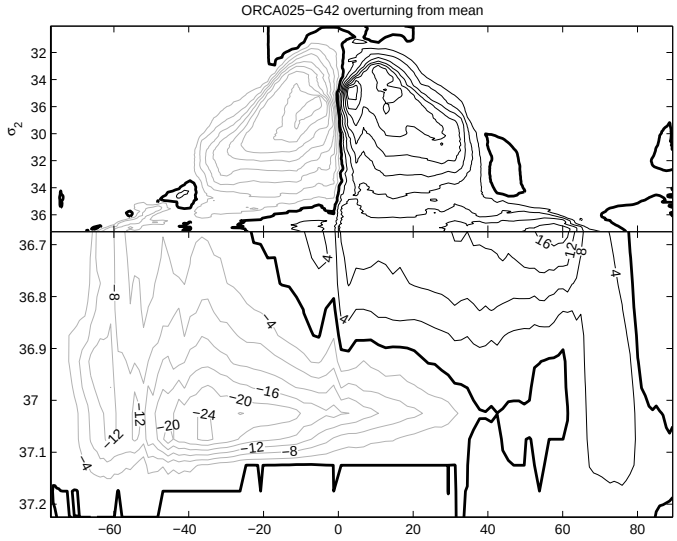

Figure 4: Global overturning in σ_2-coordinates calculated from the average density and velocity of years 8-10 of ORCA025-G42.

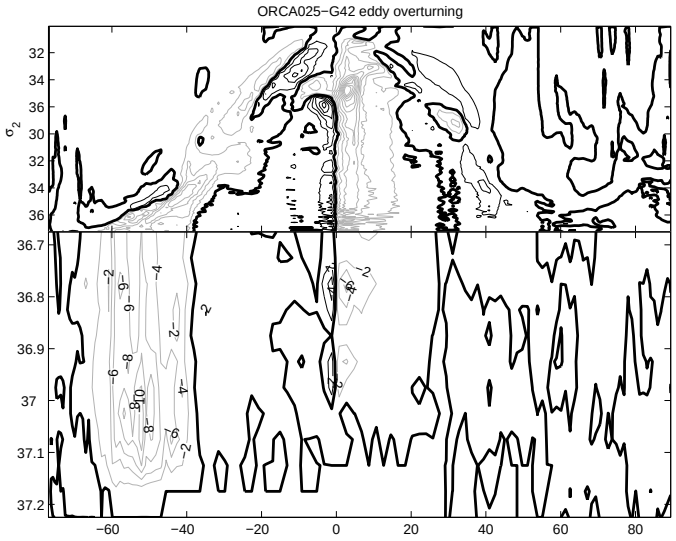

Figure 5: Eddy contribution to global overturning in σ_2-coordinates (difference of the two previous figures). Contour interval is 2 Sv.

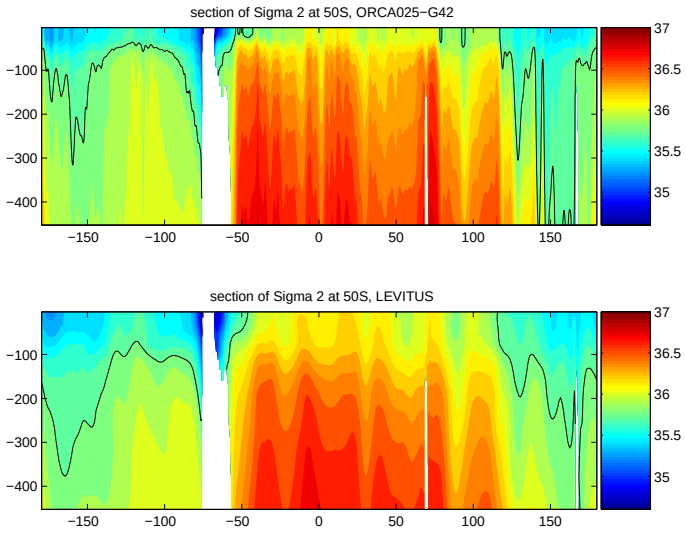

Figure 6: Density section (σ_2) at 50°S in the top layer of the ORCA025-G42 model (top) and in the Levitus climatology (bottom). The black contour represent the $\sigma_2 = 35.8$ isopycnal.

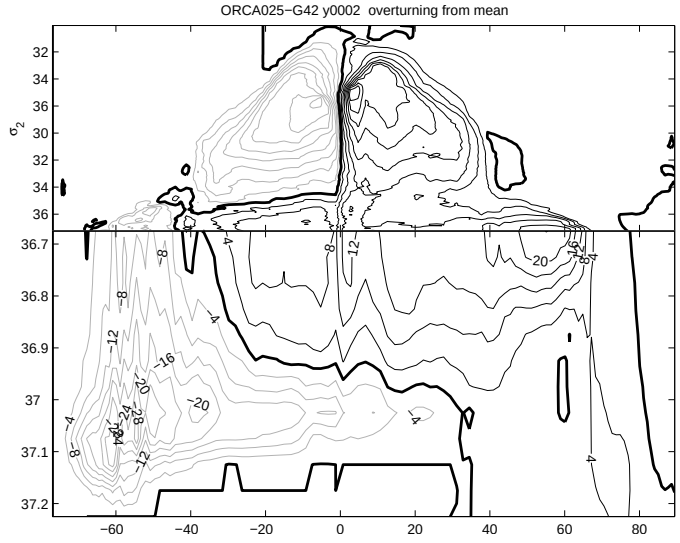

Figure 7: Global overturning in σ_2-coordinates calculated from the average density and velocity of year 2 of ORCA025-G42.

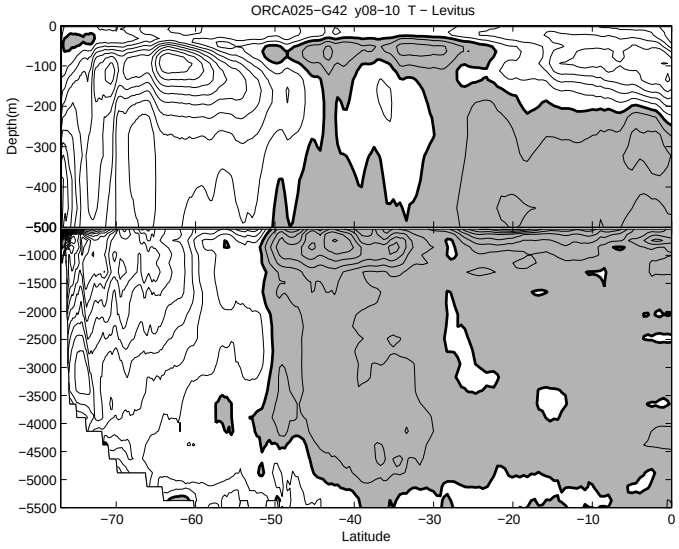

Figure 8: Zonal mean of the potential temperature difference between ORCA025-G42 (average of years 8 to 10) and the Levitus climatology. Negative values are shaded. Contour interval is 0.05 $^\circ$ for the bottom panel and 0.2 $^\circ$for the top panel.

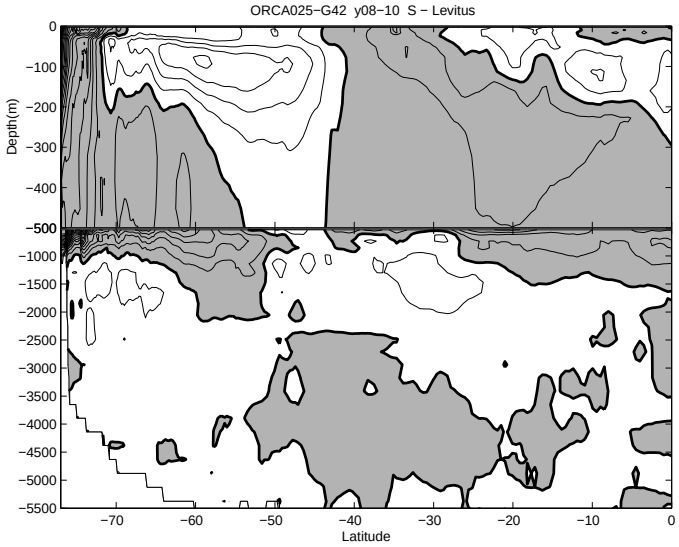

Figure 9: Zonal mean of the salinity difference between ORCA025-G42 (average of years 8 to 10) and the Levitus climatology. Negative values are shaded. Contour interval is 0.01 Psu for the bottom panel and 0.05 PSU for the top panel.

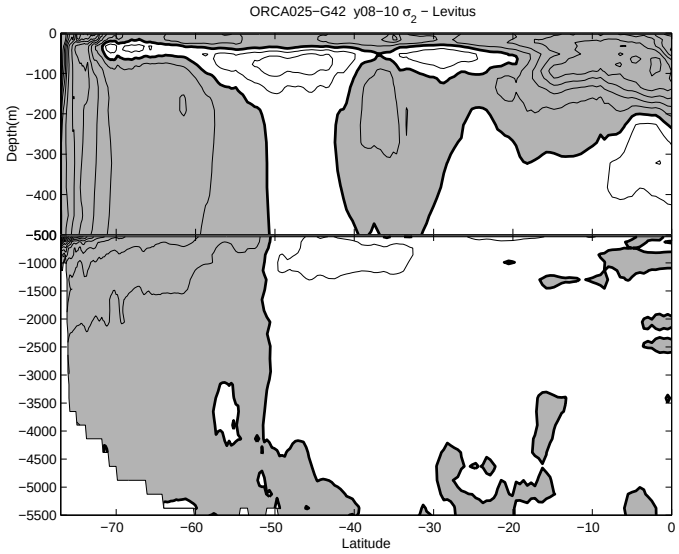

Figure 10: Zonal mean of the density (σ_2) difference between ORCA025-G42 (average of years 8 to 10) and the Levitus climatology. Negative values are shaded. Contour interval is 0.025 kg.m^{-3} for the bottom panel and 0.05 kg.m^{-3} for the top panel.

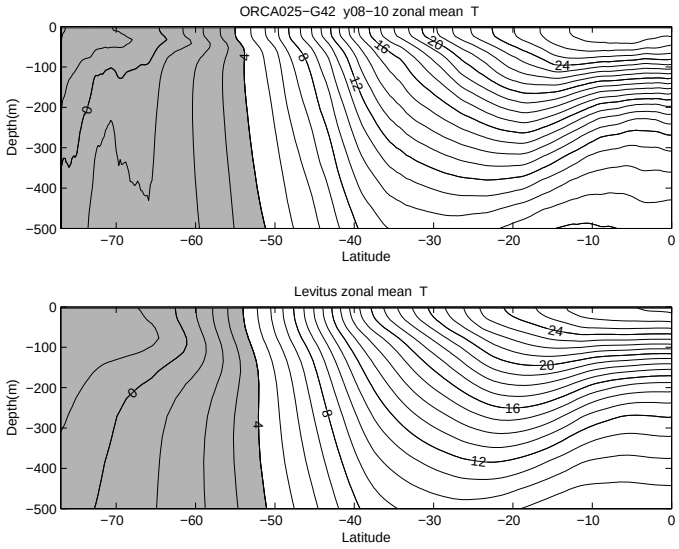

Figure 11: Zonal mean profiles of potential temperature in the upper 500 m for ORCA025-G42 (top) and Levitus (bottom). Temperatures lower than 4° are shaded.

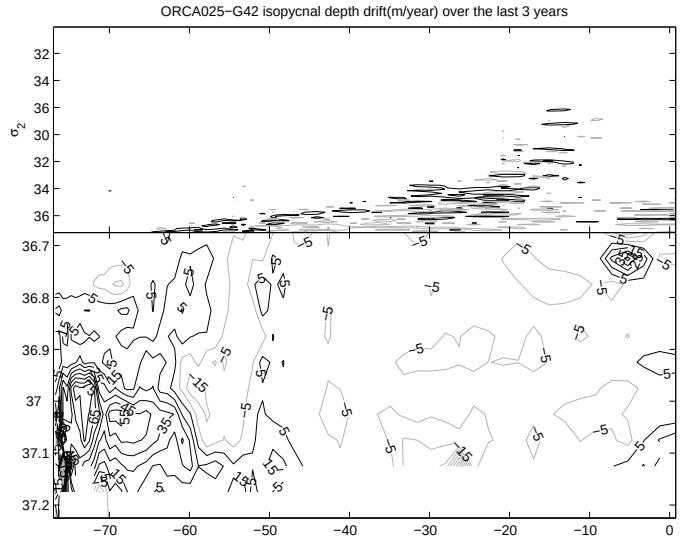

Figure 12: Drift in isopycnal depth (m/year), over the last 3 years of the model run, as a function of σ_2 density. Positive values indicate isopycnals moving downward.

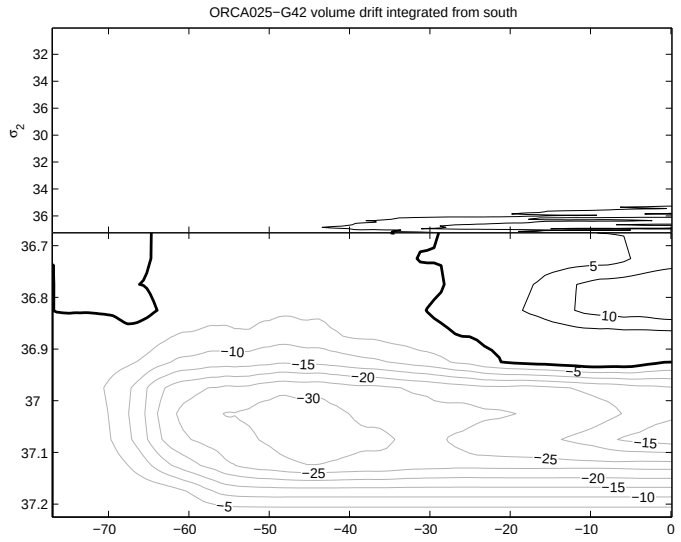

Figure 13: Drift in volume integrated from the bottom and from the south (Sv).

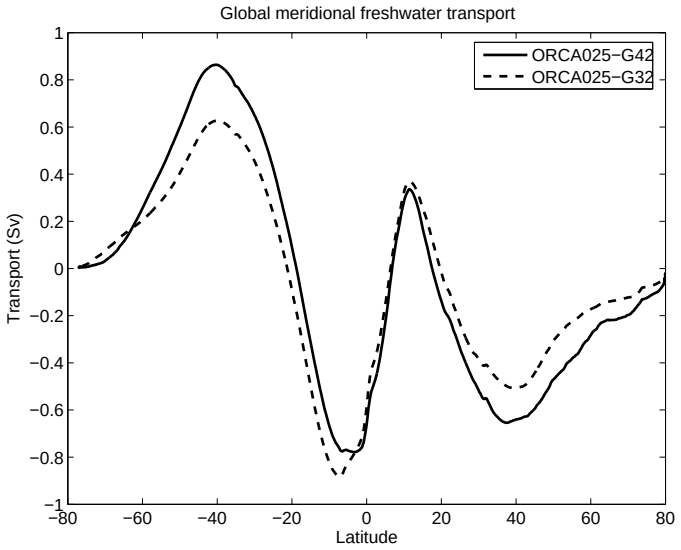

Figure 14: Meridional water transport for ORCA025-G32 and G42. The freshwater transport implied by the surface surface flux (with global mean removed) is not plotted because it undistinguishable from the model transport on this scale (the difference is of order 1%).

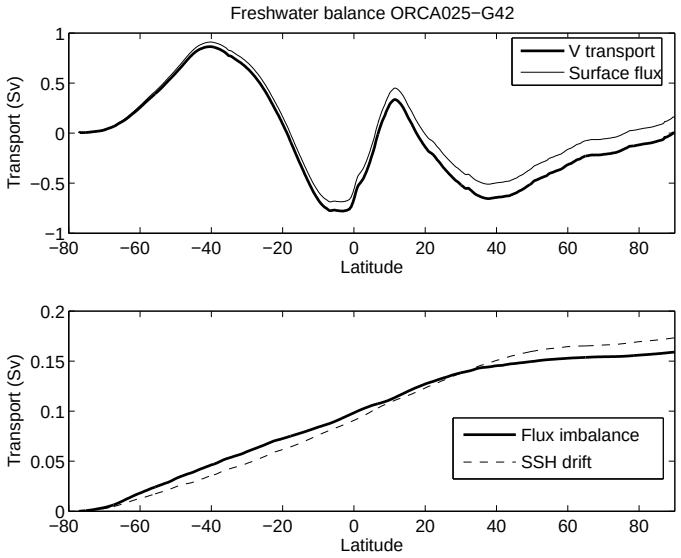

Figure 15: Water balance in ORCA025-G42. Top graph: meridional water transport, and transport implied by surface water flux (without removing the zonal mean). Bottom panel: the imbalance between the two curves compared with the integral of the drift in sea surface height.

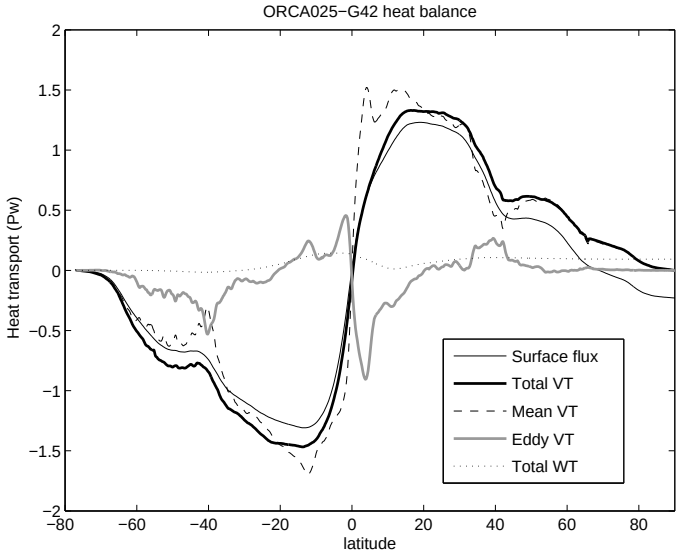

Figure 16: Terms of the heat balance for ORCA025-G42: transport implied by the surface flux, total meridional transport, with its mean and eddy components, and vertical component wT.

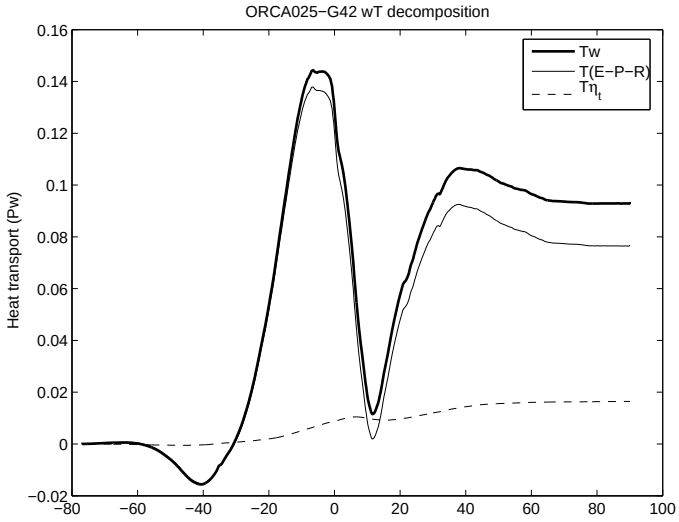

Figure 17: Decomposition of the vertical flux wT (see (5) in the text for details).

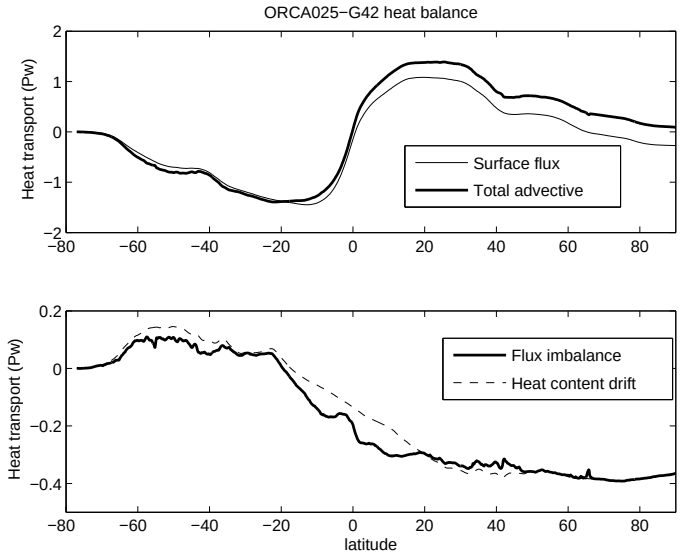

Figure 18: Heat balance for ORCA025-G42 over 3 years. Top panel: transport implied by the surface flux and total advective transport (including the wT term). Bottom: the flux imbalance (difference between the two curves in the top panel) compared with the heat content drift integrated from the south.

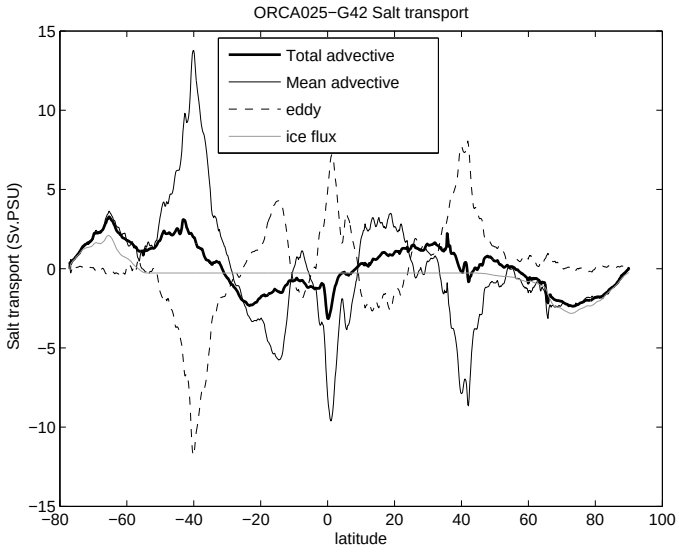

Figure 19: Meridional salt transport for experiment ORCA025-G42, years 8 to 10.

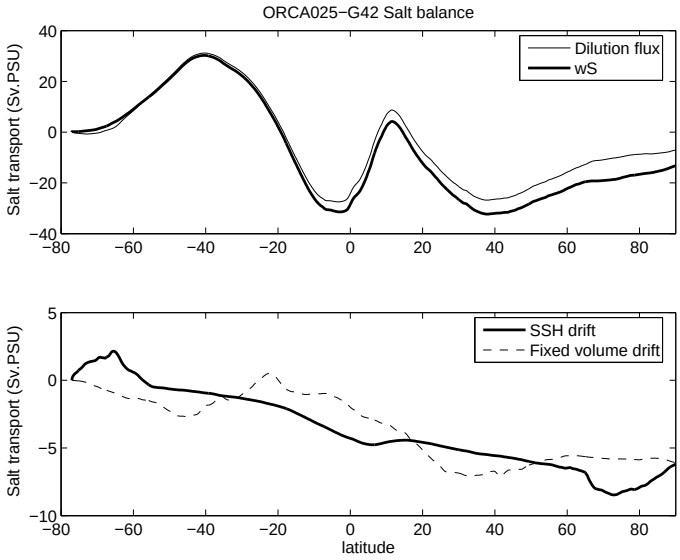

Figure 20: Salt balance for ORCA025-G42. Top panel: transport implied by the surface flux and wS term. Bottom: the flux imbalance (difference between the two curves in the top panel) compared with the salt content drift integrated from the south.